# Thoracic ultrasound strain elastosonography as non-invasive biomarker of COPD-associated lung injury: a feasibility study

Antonio Nouvenne[a], Ilaria Zanichelli[b], Nicoletta Cerundolo[a], Gianluca Milanese[b,c], Nicola Sverzellati[b,c], Martina Rendo[d], Erminia Ridolo[a,b], Simone Scarlata[e], Tiziana Meschi[a,b], Andrea Ticinesi[a,b]

[a] Geriatric-Rehabilitation Department, Azienda Ospedaliero-Universitaria di Parma, Parma, Italy

[b] Department of Medicine and Surgery, University of Parma, Parma, Italy

[c] Diagnostic Department, Azienda Ospedaliero-Universitaria di Parma, Parma, Italy

[d] Primary Care Department, Parma District, Azienda Unità Sanitaria Locale di Parma, Parma, Italy

[e] Unit of Respiratory Pathophysiology and Thoracic Endoscopy, Campus Bio Medico University and Teaching Hospital, Rome, Italy

**Short title:** Thoracic strain elastosonography in COPD

*Corresponding author:
Dr. Andrea Ticinesi, M.D. Ph.D.
Department of Medicine and Surgery, University of Parma, Via Antonio Gramsci 14, 43126 Parma, Italy
e-mail: andrea.ticinesi@unipr.it
Phone: +39 0521 703871; Mobile: +39 3471845191; Fax: +39 0521702383
ORCID-ID: 0000-0001-9171-8592

**Main text word count:** 3153; **Figures:** 3; **Tables:** 1; **References:** 38

**KEY WORDS**: elastography; chest ultrasound; COPD; lung injury; stiffness.

**ABSTRACT**

**Background-** Transthoracic strain elastosonography (TSE) is being increasingly studied for estimating lung-pleura interface stiffness in pulmonary fibrosis. To date, no data exist on its application in chronic obstructive pulmonary disease (COPD).

**Objectives-** To describe the TSE pattern in patients with COPD and healthy subjects, either smokers or non-smokers, and evaluate the feasibility of this technique for early detection of COPD in smokers.

**Methods-** Nineteen patients with COPD, twenty-one healthy smokers and twenty healthy non-smokers underwent spirometry and TSE. Elastosonography was performed by one ultrasound-certified operator on 12 different scans for each participant, on right and left side, anteriorly and posteriorly, on upper and lower lobes. For each scan, lung-pleura interface stiffness index (SI) was calculated, and the average SI on all 12 scans (SI-12) and on posterior basal scans (SI-PB) was calculated and used for comparisons among groups of participants and correlations with spirometric parameters.

**Results-** Patients with lung injury (i.e., with COPD or healthy smokers) exhibited significantly increased lung-pleura interface stiffness on TSE, measured by SI-12 and SI-PB, than healthy non-smokers ($P<0.05$). Unlike SI-12, SI-PB was able to discriminate between subjects with lung injury and healthy non-smokers on Receiver Operating Characteristics analysis (Area Under the Curve 0.846, 95% Confidence Interval 0.730-0.926, $p<0.001$), and correlated with Forced Expiratory Volume in the first second ($r=-0.31$, $p=0.018$).

**Conclusion-** The measurement of lung-pleura interface stiffness by TSE in posterior basal scans was able to discriminate patients with lung injury from healthy non-smokers. The role of TSE for detecting early lung damage in COPD should be further investigated.

## INTRODUCTION

Elastosonography is an ultrasound technique that provides an in-vivo non-invasive assessment of tissue elasticity. It is being increasingly used within daily clinical practice in various fields of medicine, helping clinicians to assess the alterations of tissue elasticity related to cancer or inflammatory diseases, especially in breast, liver and prostate imaging [1-2].

Two types of elastosonography are available, namely shear-wave elastosonography (SWE) and strain elastosonography (SE) [1]. SWE is based on the emission of high-energy acoustic pulses from the ultrasound probe inducing waves of compression in the examined tissues that, in turn, produce shear waves that are detected by the probe. Conversely, in SE compression of the examined area is directly performed by the operator. A color-coded image differentiates tissue elasticity, with colors ranging between two extremes typically represented by blue (maximal stiffness) and red (maximal elasticity) [1-2].

The technique relies on the assumption that the examined tissue is elastic, incompressible and isotropic [3]. This ideal model cannot be perfectly applied to the physics of soft tissues, where elasticity, compressibility and isotropy are violated in several conditions [3]. This is particularly true for the lung tissue, whose elastosonographic examination may be particularly challenging, from a technical perspective, because a direct vibration excitation on the lung surface is not possible and the surface wave propagation on the lungs must be obtained by vibration excitation applied on the chest wall [4].

In spite of this, SWE and SE are increasingly being studied in the field of respiratory medicine. Apart from application of SWE during endobronchial ultrasound-guided transbronchial needle aspiration (EBUS-TBNA) procedures for differentiating malignant versus non-malignant consolidations and mediastinal and hilar lymph nodes [5-9], transthoracic SWE was also shown to be of potential utility in discriminating between subpleural malignant lesions from non-malignant consolidations [10-12]. Furthermore, the pioneering studies by Zhang and colleagues has shown that the lung tissue, despite its low density and very high acoustic impedance, can generate a surface wave propagation at the

lung-pleura interface that can be reliably and reproducibly measured by elastosonography in both healthy subjects [13] and patients with interstitial lung disease [14-16]. In these conditions, the prevalent subpleural distribution of lung abnormalities makes shear waves more easily detectable by ultrasound probes. Recent studies have also reported promising data on the application of elastosonography in pulmonary edema [17] and COVID-19 pneumonia [18]. To date, transthoracic lung elastosonography has not been studied in patients with chronic obstructive pulmonary disease (COPD) yet. Although the distribution of lesions in COPD is not exclusively subpleural, significant changes in comparison with normal lung tissue density at the pleural interface are anyway expected, due to smoke-induced remodeling in peripheral airways (increased tissue density) or secondary to emphysema (reduced density) [19]. Computed tomography (CT) studies have also shown that pulmonary stiffness was increased from the early phases of the disease [20].

Thus, we hypothesized that transthoracic SE can discriminate between subjects suffering from COPD and healthy non-smokers and provide a measurement of increased lung-pleura interface stiffness in long-time smokers not yet diagnosed with COPD. Currently, early COPD imaging biomarkers are not routinely tested within daily clinical practice [21-23], and lung-pleural interface stiffness, measured by transthoracic SE, could theoretically represent an early marker of COPD-associated lung injury. The aim of this pragmatic, proof-of-concept, cross-sectional study was therefore to describe the transthoracic elastosonographic pattern in these three categories of subjects and evaluate its feasibility as a tool for early detection of COPD.

## METHODS

### *Study design, population and setting*

Sixty participants were enrolled in this cross-sectional, pragmatic diagnostic study, divided in three categories:

a) Group A: patients with confirmed spirometric diagnosis of COPD and no recent exacerbation.

b) Group B: healthy subjects with smoking history (either ongoing or former, ≥ 10 pack-years) and normal spirometry.

c) Group C: healthy non-smokers.

Each participant provided informed consent in written form. Excluded subjects were those with alpha-1 antitrypsin deficiency, severe respiratory failure, cognitive impairment, severe disability, neurological illness preventing compliance to examinations, heart failure, severe generalized edema, or cancer.

The study was conducted in an Internal Medicine unit of a large academic hospital, in which the use of point-of-care thoracic ultrasound is commonplace for the management of patients with respiratory illness [24-25].

The study protocol was approved by the local Ethics Committee and registered on ClinicalTrials.gov (NCT04149652).

### *Clinical procedures and assessment of respiratory functions*

Each participant was screened for inclusion through a careful physical examination and evaluation of medical history. Spirometry was performed with a JAEGER™ MasterScope Body cabin, unless the participant had already undergone such examination for clinical reasons within the previous month. COPD diagnosis was made on clinical-instrumental basis (i.e. by integration of spirometric data with clinical and anamnestic records). Thus, clinical-anamnestic data, Forced Expiratory Volume in the first second ($FEV_1$), the ratio between $FEV_1$ and Forced Vital Capacity ($FEV_1$/FVC, Tiffeneau Index),

were the basis for classifying participants in groups a), b) or c). The Maximal Mid-Expiratory flow between 25% and 75% ($MMEF_{25-75}$) was also considered as a proxy of obstructive small airway disease.

***Lung ultrasound and strain elastosonography procedures***

A portable ultrasound equipment, with convex 3.5-5 MHz and linear 4-8 MHz probes (Esaote MyLab Alpha™, Esaote, Genova, Italy), was used for all ultrasound and elastosonographic examinations. One operator with more than five years of experience and certification in thoracic ultrasonography performed all the examinations.

First, each participant was examined in the sitting position with B-mode ultrasound using a convex probe, following a protocol of visualization of all lung fields used for the diagnosis of acute respiratory diseases [24-25]. The probe was moved longitudinally on parasternal, hemiclavicular, axillary, scapular, and paravertebral lines, and then transversally in intercostal spaces, to evaluate the ultrasound characteristics of pleural line and subpleural lung parenchyma and exclude the presence of unknown underlying abnormalities that could impair elastosonographic examination.

Then, the probe was positioned posteriorly on the right lung basis, two intercostal spaces above the diaphragm. The SE function was activated with the duplex mode, that allows to visualize on screen both B-mode and elastosonography images. Then, the operator executed gentle and rhythmic manual compressions with the convex probe on the thoracic wall, following the indications suggested by the compression sensor of the ultrasound probe. To optimize SE image quality, the window of the ultrasonographic region of interest (ROI) was reduced to analyze the entire vertical extension of the thoracic surface and make it appear as red, meaning that compressions were applied properly (Figure 1A). The two lateral thirds of the image were excluded from the ROI, to avoid analyzing echoes from marginal structures such as the column or the ribs (Figure 1A). The SE image was then saved on the ultrasound software for further processing and analysis.

Twelve different elastosonographic scans were obtained in each participant, six for each lung:

- basal and apical on the scapular line;
- basal and apical on the anterior axillary line;
- basal and apical on the hemiclavicular line.

Basal scans were obtained two intercostal spaces above the diaphragm. Apical scans were obtained in the third intercostal space, except for the left scan on the hemiclavicular line, that was obtained in the first or second intercostal space to avoid the cardiac region.

***Analysis of elastosonographic images***

Elastosonographic images were analyzed with the ElaXto™ software provided by the ultrasound manufacturer (Esaote, Genova, Italy) [1]. This software measures the percentage of tissue stiffness deviating from a pre-specified stiffness threshold (set at 20%), in accordance with the chromatic range of the elastosonographic image. The obtained Stiffness Index (SI) was a measurement of stiffness ranging from 0 (lower stiffness threshold) to 100 (maximal stiffness). The software allows to calculate the SI in a specific ROI that is selected by the examiner.

For the purposes of this study, the ROI was first identified as the entire area under the pleural line included in the image (Figure 1A), and then was reduced to cover both the upper (3-4 cm of depth from pleural line) (Figure 1B) and lower part of the image (Figure 1C).

In aerated lungs, only the part of the image immediately beyond the pleural line (upper part of the image) corresponds to signals truly generated at the lung-pleural interface, while the lower part of the image could instead represent the result of reverberation artifacts amplifying the signal produced at the lung-pleural interface [26]. Thus, the measure of SI in the lower parts of elastosonographic images may not correspond to the true lung parenchyma stiffness. However, it may represent a useful parameter for differentiating normal and diseased lungs as well. Therefore, for clinical purposes, we calculated the average of upper and lower SI values of all twelve scans (SI-12, representing the average of SI for the 12 scans). We also calculated the average of SI values obtained in right and left posterior basal scans (SI-PB), and in right and left apical scans (SI-PA).

***Statistical analysis***

Data were expressed as median and interquartile range (IQR) for continuous variables or as percentage for dichotomous variables. The demographic (age, gender), spirometric ($FEV_1$, Tiffeneau Index) and elastosonographic metrics (SI-12, SI-PB, SI-PA) were compared among the three study groups with Kruskal-Wallis or chi-square test, as appropriate. The correlations of elastosonographic parameters with age, $FEV_1$ and Tiffeneau Index were also assessed in the whole study population with Spearman's rank correlation coefficients.

The capacity of elastosonographic indexes (SI-12, SI-PB, SI-PA) to discriminate between healthy never smokers (group C) and patients with COPD (group A), and between group C and subjects with lung injury (healthy smokers plus patients with COPD, groups A and B) was also assessed through Receiver Operating Characteristics (ROC) curve analysis and calculation of the Area Under the ROC Curve (AUC).

All analyses were performed with Stata v.16 (StataCorp LLC, College Station, Texas, US), considering P values $<0.05$ as statistically significant.

## RESULTS

Among sixty participants, nineteen (31.7%; 13 M, 6 F) were included in Group A, twenty-one (35%; 13 M, 8 F) in Group B, and twenty (33.3%; 10 M, 10 F) in Group C. No age and gender distribution differences were detected, while $FEV_1$ and Tiffeneau Index were lower ($p<0.001$) in Group A (Table 1).

The typical elastosonographic image pattern of each group is depicted in Figure 2. Blue nuances were more frequent in group A at visual inspection, while red nuances prevailed in images from participants categorized in group B and C. Further images are provided in Supplementary Material.

A trend towards increased SI-12 values was detected from Group C to Group A (Group A: median 53.71, IQR 52.43-55.24; Group B: median 52.74, IQR 51.66-56.95; Group C: median 52.26, IQR 49.10-53.61; p=0.031) (Table 1). SI-12 discriminated between Group A and Group C on ROC analysis (AUC 0.672, 95% CI 0.539-0.788, p=0.014) (Figure 3A). However, SI-12 was not significantly correlated with any of the spirometric parameters considered in the investigation ($FEV_1$: r=-0.14, 95% CI -0.39 to 0.11, p=0.266; Tiffeneau Index: r=-0.19, 95% CI -0.42 to 0.07, p=0.151; $MMEF_{25-75}$ r=-0.03, 95% CI -0.30 to 0.25, p=0.841) .

SI-PB showed higher values in Group B (healthy individuals with smoking history) than in Group A (patients with COPD), while Group C (healthy never smokers) had the lowest average values of this variable (Group A: median 53.97, IQR 52.29-58.81; Group B: median 55.65, IQR 50.65-58.51; Group C: median 49.09, IQR 47.65-51.65; p<0.001) (Table 1). SI-PB significantly discriminated patients with lung damage (either COPD or smoke-induced damage, Groups A and B) from healthy never smokers (Group C) on ROC analysis (AUC 0.846, 95% CI 0.730-0.926, p<0.001; Figure 3B). In the studied population, SI-PB was also significantly and inversely correlated with $FEV_1$ (r=-0.31, 95% CI -0.52 to -0.05, p=0.018), but not with Tiffeneau Index (r=-0.16, 95% CI -0.40 to 0.09, p=0.209) or $MMEF_{25-75}$ (r=-0.25, 95% CI -0.49 to 0.03, p=0.07).

SI-PA was not statistically different among the three groups of participants (Table 1).

## DISCUSSION

In this proof-of-concept study, the qualitative appearance of transthoracic SE showed different patterns among healthy never smokers, smokers with normal respiratory function and patients with COPD. These differences were also reflected by SI, in particular when calculated from the posterior basal scans. Moreover, SI-PB exhibited a fairly good correlation with $FEV_1$ and could discriminate between participants with and without lung injury.

Overall, these results support the feasibility of transthoracic SE for non-invasive detection of subpleural lung damage in subjects who are at risk for COPD. In the pathogenesis of COPD, lung tissue alterations generally precede pathological findings on respiratory function tests, as well as the onset of respiratory symptoms [23]. The detection of emphysema, bronchial wall thickness and air trapping on chest CT scans of healthy individuals is associated with increased risk of developing overt forms of COPD, representing a subclinical marker of the disease [27]. In recent years, several studies have investigated the possible role of chest imaging, particularly low-dose CT, for screening the general population for early diagnosis of COPD or lung cancer [20-23, 28].

These studies, however, were not focused on lung elasticity, which is affected since the earliest stages of COPD. Interestingly, Hasse and colleagues [29] validated a measure of lung tissue elasticity derived from 4-dimensional computed tomography (4DCT) scans. This parameter exhibited a good correlation between respiratory function and severity of COPD in 13 patients with coexisting COPD and lung cancer [29]. However, the methodology of assessment of lung elasticity with chest CT requires 4DCT technology, which is not easily available and implies a higher exposure to ionizing radiations. One further approach based on elastic registration of CT scans was focused on the detection of morphological and functional changes in patients with systemic sclerosis-related interstitial lung disease [30].

On the other hand, transthoracic SE is a non-invasive and radiation-free technique. To date, this technique has been studied mainly in the context of lung fibrosis, either idiopathic or caused by systemic autoimmune disorders [14-16]. In these conditions, the increase in lung-pleura interface

stiffness is more obvious and directly correlated with the disease stage and severity [14-16]. In a recent study conducted on 77 subjects, embedding elastosonographic measures of stiffness with functional parameters in an algorithm for assessment of lung fibrosis, elastosonography increased the overall diagnostic accuracy [31]. Anecdotal evidence also suggests that transthoracic elastosonography might estimate the severity of lung involvement in COVID-19 pneumonia [18] and help for the differential diagnosis of lung parenchymal lesions with complicated morphology [32].

To the best of our knowledge, our study is the first assessing the role of transthoracic SE in COPD, as well as its potential role as marker of early damage in healthy smokers without spirometric evidence of obstructive pattern. Future studies with larger sample size and longitudinal design are awaited to investigate whether the alterations of SI predict deterioration of respiratory function with development of obstructive pattern and COPD. Comparison of elastosonography with low-dose chest CT would also allow to establish whether lung-pleura interface stiffness measured by elastosonography might increase the diagnostic value of traditional imaging in early detection of at risk patients.

Despite the promising findings, some pitfalls emerging from this proof-of-concept investigation should be carefully considered. First, SI-12, SI-PB and SI-PA do not represent direct measures of lung parenchyma stiffness, but only an estimation of stiffness at the lung-pleura interface, since deep structures cannot be directly assessed by thoracic ultrasound when the lungs are normally aerated and the pleura is not involved [26]. Furthermore, the differences of SI-12 among the groups of participants were only mild in absolute terms, and probably of little clinical value. The capacity of SI-12 of discriminating patients with COPD from healthy participants was also poor (Figure 3A). The derivation of the SI-12 parameter was also very time-consuming, requiring the execution of 12 ultrasound scans and the subsequent analysis of several images in the post-processing phase. SI-12, being the average of the SI measured in different scans, may not adequately account for regional variations of the distribution of emphysematous lesions, which is common since the early phases of COPD and influenced by genetic factors [33-34].

SI-PB, instead, was faster and simpler to obtain, requiring only two ultrasound scans and the analysis of a small number of images. SI-PB specifically explores the presence of lower lobe lung-pleura interface alterations, which are generally associated with increased clinical severity at the time of COPD diagnosis, but with reduced risk of clinical progression to severe respiratory failure in comparison with upper lobe emphysema [35-36]. Although in our study SI-PB was associated with an excellent capacity of discriminating healthy non-smokers from subjects with lung injury, these aspects of the pathophysiology of COPD should be considered for a correct interpretation of its significance.

Of note, the quality of transthoracic SE examinations could be reduced in older patients, due to several reasons, including difficulties in maintaining the sitting position, age-related changes of lung and chest wall anatomy, presence of comorbidities (e.g., obesity) that could pose challenges in obtaining elastosonographic images of adequate quality [37]. All these elements could have influenced the results of our study, that was conducted on a relatively small sample of subject mostly older than 70 years.

Additional limitations of our study include its cross-sectional design and the lack of data on chest CT. The use of the SE, instead of SWE, could be also regarded as a limitation, because it is less standardized in its application and more dependent on the examiner's manual skills. Previous studies on lung elastosonography mainly used SWE rather than SE, but the examinations were made mainly in experimental conditions and not in a clinical setting [14-17]. SE, instead, is a widely used technique with a good diagnostic value in other fields of medicine, and represents a good compromise for a quick assessment at the patient's bedside, being more accessible as a complement of routine lung ultrasound tests. Unfortunately, no measures of inter- and intra-operator variability were taken in our study. However, data from breast SE indicate that the process of image acquisition is only fairly affected by intra- and inter-operator variability, while the critical step relies in image interpretation [38]. The use of the custom software ElaXto™ in our study may favor repeatability of results. Finally, having been conceived with a proof-of-concept design, the study lacked sufficient power to detect

possible differences in elastosonographic pattern and lung-pleura interface stiffness index among patients with different COPD severity.

Despite these limitations, the results of this investigation point out that the assessment of lung-pleura interface stiffness by transthoracic elastosonography represents a promising marker of early COPD lesions. The presence of increased stiffness on lung-pleura interface in healthy smokers could in fact precede the onset of alterations in respiratory function tests and represent an early stage of lung injury associated with COPD. Thus, lung elastosonography should be further studied for its potential applications in the field of screening and diagnosis of COPD.

## CONCLUSIONS

The measurement of lung-pleura interface stiffness by transthoracic SE, especially in posterior basal regions, was able to discriminate patients with COPD and subjects with smoke-related lung injury from healthy non-smokers. The use of this technique should be further investigated for its potential utility in screening and early detection of COPD.

**Acknowledgements**

The authors wish to thank Dr. Giulia Mori and Dr. Maria Letizia Catalano for their contribution in the development of the elastosonographic protocol for lung assessment. They also wish to thank Dr. Maria Cristina Nizi, Dr. Paola Kihlgren and Dr. Francesco Pucciarini for the spirometric assessment of study participants.

**Statement of Ethics**

The study protocol was approved by the Ethics Committee of Area Vasta Emilia Nord, Emilia-Romagna Region, under the ID 614/2018/DISP/AOUPR. The study was conducted in accordance with the Declaration of Helsinki.

**Informed consent**

Obtained from all participants in written form before enrolment.

**Disclosure statement**

The authors have no conflict of interest to declare.

**Funding sources**

This study was supported by a grant from the Cariparma Foundation (Fondazione Cariparma), awarded to Prof. Tiziana Meschi for the implementation of bedside thoracic ultrasound techniques at the Geriatric-Rehabilitation Department of Parma University-Hospital.

**Trial Registration**

ClinicalTrials.gov ID: NCT04149652.

## Author contribution

Antonio Nouvenne: conceptualization, investigation, data interpretation, manuscript revision for substantial content; Ilaria Zanichelli: investigation, data interpretation, manuscript revision for substantial content; Nicoletta Cerundolo: investigation, manuscript revision for substantial content; Gianluca Milanese: data interpretation, formal analysis, manuscript revision for substantial content; Nicola Sverzellati: formal analysis, manuscript revision for substantial content; Martina Rendo: data interpretation, manuscript revision for substantial content; Erminia Ridolo: supervision, manuscript revision for substantial content; Simone Scarlata: data interpretation, manuscript revision for substantial content; Tiziana Meschi: supervision, manuscript revision for substantial content; Andrea Ticinesi: conceptualization, investigation, data interpretation, manuscript drafting.

## Data availability statement

The dataset of the study is not publicly available, due to restrictions imposed by personal data treatment regulations. Anonymized data can be however made available by the corresponding author upon reasonable request.

**REFERENCES**


1. Sigrist RMS, Liau J, El Kaffas A, Chammas MC, Willmann JK. Ultrasound elastography: review of techniques and clinical applications. Theranostics. 2017;7(5):1303-1329.
2. Gennisson JL, Deffieux T, Fink M, Tanter M. Ultrasound elastography : principles and techniques. Diagn Interv Imaging 2013;94(5):487-495.
3. Bamber J, Cosgrove D, Dietrich CF, Fromageau J, Bojunga J, Calliada F, et al. EFSUMB guidelines and recommendations on the clinical use of ultrasound elastography. Part 1: Basic principles and technology. Ultraschall Med2013;34(2):169-184.
4. Zhou B, Yang X, Zhang X, Curran WJ, Liu T. Ultrasound elastography for lung disease assessment. IEEE Trans Ultrason Ferroelectr Freq Contr. 2020;67(11):2249-57.
5. Dietrich CF, Jenssen C, Herth FJF. Endobronchial ultrasound elastography. Endosc Ultrasound. 2016;5:233-8.
6. Nakajima T, Inage T, Sata Y, Morimoto J, Tagawa T, Suzuki H, et al. Elastography for predicting and localizing nodal metastases during endobronchial ultrasound. Respiration. 2015;90-499-506.
7. Fujiwara T, Nakajima T, Inage T, Sata Y, Sakairi Y, Tamura H, et al. The combination of endobronchial elastography and sonographic findings during endobronchial ultrasound-guided transbronchial needle aspiration for predicting nodal metastases. Thorac Cancer. 2019;10:2000-5.
8. Verhoeven RLJ, Trisolini R, Leoncini F, Candoli P, Bezzi M, Messi A, et al. Predictive value of endobronchial ultrasound strain elastography in mediastinal lymph node staging: the E-Predict multicenter study results. Respiration. 2020;99:484-92.
9. Gompelmann D, Kontogianni K, Sarmand N, Kaukel P, Krisam J, Eberhardt R, et al. Endobronchial ultrasound elastography for differentiating benign and malignant lymph nodes. Respiration. 2020;99:779-83.

10. Kuo YW, Chen YL, Wu HD, Chien YC, Huang CK, Wang HC. Application of transthoracic shear-wave ultrasound elastography in lung lesions. Eur Respir J. 2021;57:2002347.
11. Quarato CMI, Venuti M, Dimitri L, Lacedonia D, Simeone A, Mirijello A, et al. Transthoracic ultrasound shear wave elastography for the study of subpleural lung lesions. Ultrasonography. 2022;41:93-105.
12. Boccatonda A, Susca V, Primomo GL, Cocco G, Cinalli S, Di Resta V, et al. Role of shear-wave and strain elastography to differentiate malignant vs benign subpleural lung lesions. Medicine. 2021;100:1(e34123).
13. Zhang X, Osborn T, Zhou B, Meixner D, Kinnick RR, Bartholmai B, et al. Lung ultrasound surface wave elastography: a pilot clinical study. IEEE Trans Ultrason Ferroelectr Freq Contr. 2017;64(9):1298-304.
14. Zhang X, Zhou B, Osborn T, Bartholmai B, Kalra S. Lung ultrasound surface wave elastography for assessing interstitial lung disease. IEEE Trans Biomed Eng. 2019;66(5):1346-52.
15. Clay R, Bartholmai BJ, Zhou B, Karwoski R, Peikert T, Osborn T, et al. Assessment of interstitial lung disease using lung ultrasound surface wave elastography. A novel technique with clinicoradiologic correlates. J Thorac Imaging. 2019;34(5):313-9.
16. Zhou B, Bartholmai BJ, Kalra S, Osborn TG, Zhang X. Lung US surface wave elastography in interstitial lung disease staging. Radiology. 2019;291:479-84.
17. Wiley BM, Zhou B, Pandompatam G, Zhou J, Kucuk HO, Zhang X. Lung ultrasound surface wave elastography for assessing patients with pulmonary edema. IEEE Trans Biomed Eng. 2021;68(11):3417-23.
18. Fusco P, Di Carlo S, Petroni GM, Scimia P, Sepolvere G, Ciaschi W, et al. Lung elastosonography for diagnosis and management of COVID-19 pneumonia. Minerva Anestesiol. 2021;87(3):374-376.

19. Slater A, Goodwin M, Anderson KE, Gleeson FV. COPD can mimic the appearance of pneumothorax on thoracic ultrasound. Chest 2006;129(3):545-550.
20. Heuvelmans MA, Vonder M, Rook M, Groen HJM, De Bock GH, Xie X, et al. Screening for early lung cancer, chronic obstructive pulmonary disease, and cardiovascular disease (the Big-3) using low-dose chest computed tomography. Current evidence and technical considerations. J Thorac Imaging. 2019;34(3):160-9.
21. Stockley RA, Halpin DMG, Celli BR, Singh D. Chronic obstructive pulmonary disease biomarkers and their interpretation. Am J Respir Crit Care Med. 2019;199(10):1195-204.
22. Washko GR, Parraga G. COPD biomarkers and phenotypes: opportunities for better outcomes with precision imaging. Eur Respir J. 2018;52:1801261.
23. Xia C, Rook M, Pelgrim GJ, Sidorenkov G, Wisselink HJ, van Bolhuis JN, et al. Early imaging biomarkers of lung cancer, COPD and coronary artery disease in the general population: rationale and design of the ImaLife (Imaging in Lifelines) Study. Eur J Epidemiol 2020;35(1):75-86.
24. Ticinesi A, Lauretani F, Nouvenne A, Mori G, Chiussi G, Maggio M, et al. Lung ultrasound and chest x-ray for detecting pneumonia in an acute geriatric ward. Medicine. 2016;95(27):e4153.
25. Nouvenne A, Zani MD, Milanese G, Parise A, Baciarello M, Bignami EG, et al. Lung ultrasound in COVID-19 pneumonia: correlations with chest CT on hospital admission. Respiration. 2020;99(7):617-624.
26. Sperandeo M, Rotondo A, Guglielmi G, Catalano D, Feragalli B, Trovato GM. Transthoracic ultrasound in the assessment of pleural and pulmonary diseases: use and limitations. Radiol Med 2014;119(10):729-470.
27. Mets OM, Buckens CF, Zanen P, Isgum I, van Ginneken B, Prokop M, et al. Identification of chronic obstructive pulmonary disease in lung cancer screening computed tomography scans. JAMA. 2011;306(16):1775-1781.

28. Silva M, Milanese G, Seletti V, Ariani A, Sverzellati N. Pulmonary quantitative CT imaging in focal and diffuse disease: current research and clinical applications. Br J Radiol. 2018;91(1083):20170644.
29. Hasse K, Neylon J, Min Y, O'Connell D, Lee P, Low DA, et al. Feasibility of deriving a novel imaging biomarker based on patient-specific lung elasticity for characterizing the degree of COPD in a lung SBRT patients. Br J Radiol. 2019;91:20180296.
30. Chassagnon G, Vakalopoulou M, Régent A, Sahasrabudhe M, Marini R, Hoang-Thi TN, et al. Elastic Registration-driven Deep Learning for Longitudinal Assessment of Systemic Sclerosis Interstitial Lung Disease at CT. Radiology. 2021;298(1):189-198.
31. Zhou B, Bartholmai BJ, Kalra S, Osborn T, Zhang X, Lung mass density prediction using machine learning based on ultrasound surface wave elastography and pulmonary function testing. J Acoust Soc Am. 2021;149(2):1318-1323.
32. Lim CK, Chung CL, Lin YT, Chang CH, Lai YC, Wang HC, et al. Transthoracic ultrasound elastography in pulmonary lesions and diseases. Ultrasound Med Biol. 2017;43(1):145-152.
33. de Torres JP, Bastarrika G, Zagaceta J, Sáiz-Mendiguren R, Alcaide AB, Seijo LM, et al. Emphysema presence, severity, and distribution has little impact on the clinical presentation of a cohort of patients with mild to moderate COPD. Chest. 2011;139(1):36-42.
34. Boueiz A, Lutz SM, Cho MH, Hersh CP, Bowler RP, Washko GR, et al. Genome-wide association study of the genetic determinants of emphysema distribution. Am J Respir Crit Care Med. 2017;195(6):757-771.
35. Hoesin FAAM, van Rikxoort E, van Ginneken B, de Jong PA, Prokop M, Lammers JWJ, et al. Computed tomography-quantified emphysema distribution is associated with lung function decline. Eur Respir J. 2012;40(4):844-850.
36. Boueiz A, Chang Y, Cho MH, Washko GR, Estépar RSJ, Bowler RP, et al. Lobar emphysema distribution is associated with 5-year radiological disease progression. Chest. 2018;153(1):65-76.

37. Ticinesi A, Scarlata S, Nouvenne A, Lauretani F, Antonelli Incalzi R, Ungar A. The Geriatric Patient: The Ideal One for Chest Ultrasonography? A Review From the Chest Ultrasound in the Elderly Study Group (GRETA) of the Italian Society of Gerontology and Geriatrics (SIGG). J Am Med Dir Assoc. 2020;21(4):447-454.e6.
38. Dong Y, Zhou C, Zhou Z, Yang Z, Zhang J, Zhan W. Breast strain elastography: Observer variability in data acquisition and interpretation. Eur J Radiol. 2018;101:157-161.

## FIGURE LEGENDS

**Figure 1** – Acquisition of elastosonographic images and selection of the region of interest (ROI) for measurement of the stiffness index. A) Selection of the whole pulmonary parenchyma explored in the scan as ROI. B) Selection of the superficial portion of lung parenchyma as ROI. C) Selection of the deep portion of lung parenchyma as ROI.

**Figure 2** – Typical elastosonographic pattern of lungs of patients with COPD (A), healthy smokers (B), and healthy controls (C) on posterior basal scans. Red and yellow nuances indicate elasticity of deep tissues, while blue and green nuances indicate tissue stiffness.

**Figure 3 -** ROC curves showing the capacity of the elastosonographic stiffness index calculated as average of 12 different scans (SI-12) to discriminate between patients with COPD and healthy subjects (panel A) and the capacity of the elastosonographic stiffness index calculated as average of left and right posterior basal scans (SI-PB) to discriminate between healthy non-smokers and subjects with lung damage (healthy smokers and patients with COPD) (panel B).

**Figure 1**

A)

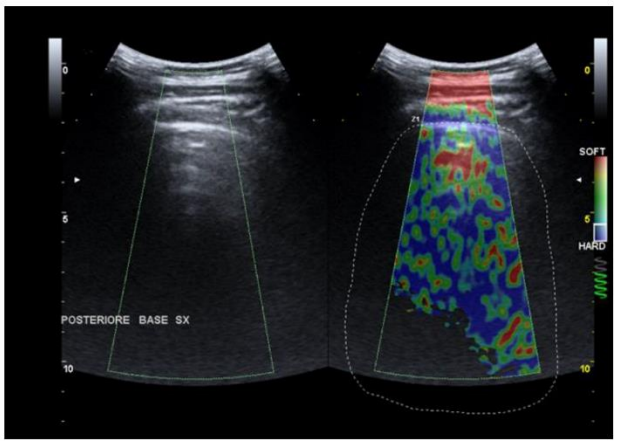
0
5
10
POSTERIORE BASE SX
Z1
SOFT
HARD
0
5
10

B)

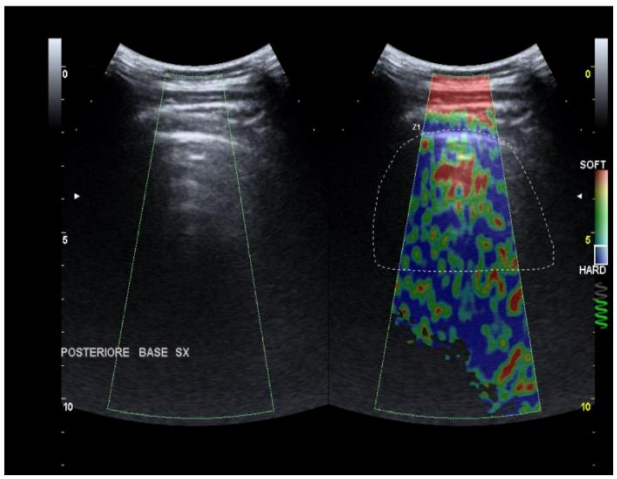
0
5
10
POSTERIORE BASE SX
Z1
SOFT
HARD
0
5
10

C)

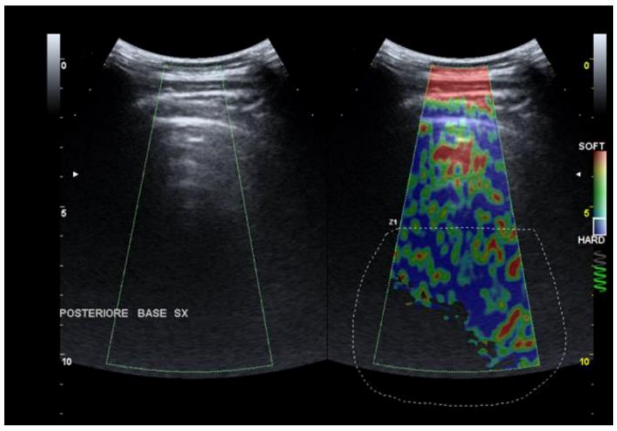
0
5
10
POSTERIORE BASE SX
Z1
SOFT
HARD
0
5
10

**Figure 2**

A)

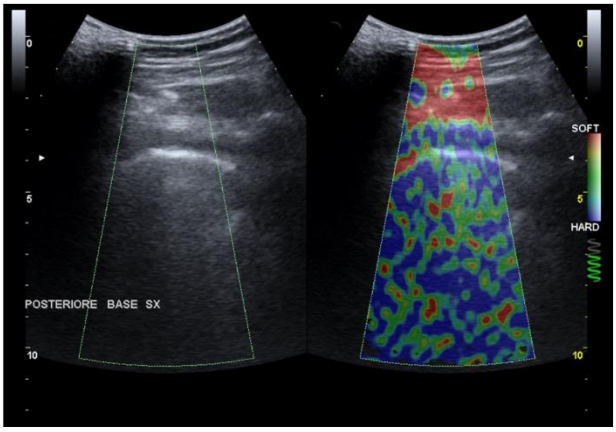
POSTERIORE BASE SX
SOFT
HARD

B)

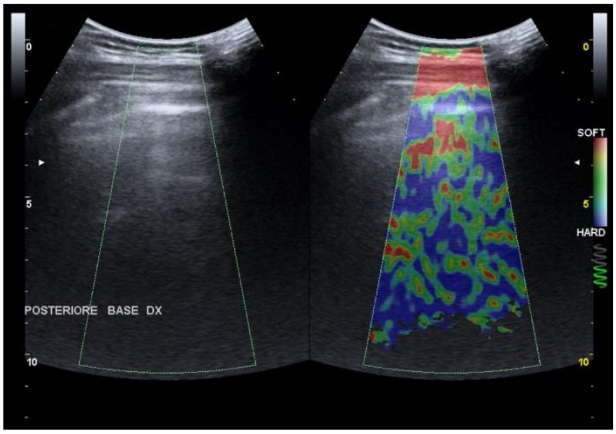
POSTERIORE BASE DX
SOFT
HARD

C)

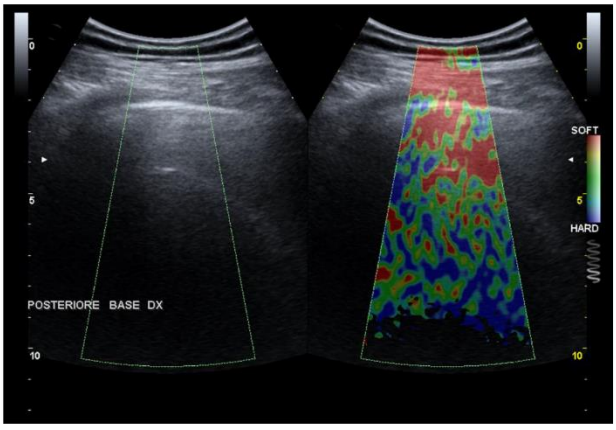
POSTERIORE BASE DX
SOFT
HARD

**Figure 3**

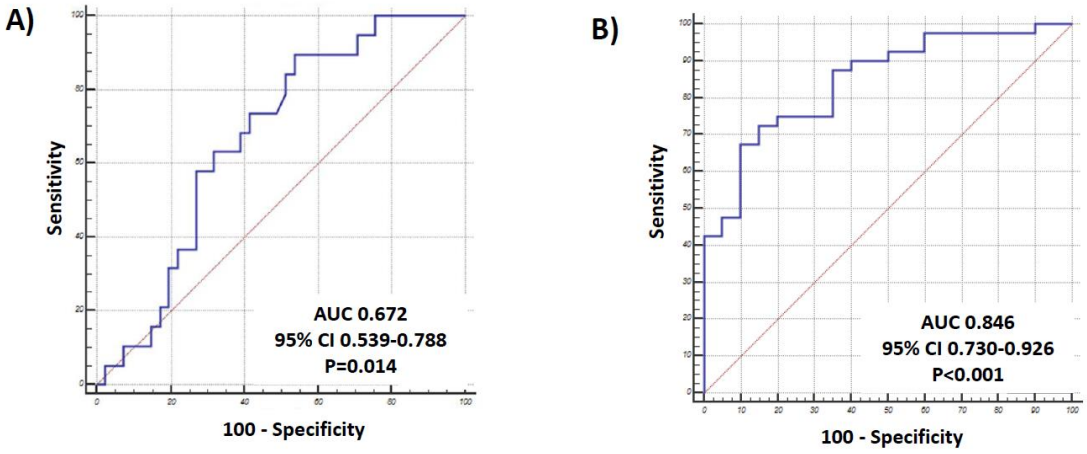
A)
Sensitivity
100 - Specificity
AUC 0.672
95% CI 0.539-0.788
P=0.014
B)
Sensitivity
100 - Specificity
AUC 0.846
95% CI 0.730-0.926
P<0.001